https://doi.org/10.48047/AFJBS.6.14.2024.11838-11861

African Journal of Biological Sciences

Journal homepage: http://www.afjbs.com

Research Paper Open Access

Pyrimidine-Benzofuran Hybrid Molecules: Synthesis, Antimicrobial Evaluation, and Molecular Docking Insights

Prasanthi Gummalla 1, Prasanthi Chitrapu 2, Balireddy Keesara 3, Rajasekhar Komarla Kumarachari 4, Kishore Bandarapalle 5, Sarad Pawar Naik Bukke 6 and Uday Kumar Nagapatla *

1 Department of Pharmaceutical Chemistry, Giet School of Pharmacy, Rajahmundry- 533296, Andhra Pradesh, India. Email: prasanthi.gummalla@yahoo.com

2 Vision College of Pharmaceutical Sciences and Research, Secunderabad-500092, Telangana, India. Email: prashantichitrapu@yahoo.com. ORCID: 0000-0002-9665-365X.

3 Department of Pharmacology, Shantiniketan College of Pharmacy, Parner, Ahmednagar-414304, Maharasthra, India. Email: brkeesara@gmail.com.

4 Department of Pharmaceutical Chemistry, Sri Padmavathi School of Pharmacy, Tiruchanur, Tirupati-517503, Andhra Pradesh, India. Email: komarla.research@gmail.com. ORCID: 0000-0001-5611-1410.

5 Department of Pharmaceutics, Sri Padmavathi School of Pharmacy, Tiruchanur, Tirupati-517503, Andhra Pradesh, India. Email: Kishore.brr89@gmail.com. ORCID: 0000-0003-0032-4331.

6 Department of Pharmaceutics and Pharmaceutical Technology, Kampala International University, Western Campus, Ishaka, Uganda. Email: drsaradpawar@kiu.ac.ug. ORCID: 0000-0002-5693-2953.

* Department of Pharmaceutical Chemistry and Analysis, MB School of Pharmaceutical Sciences (Erstwhile Sree Vidyanikethan College of Pharmacy, Tirupati-517102, Andhra Pradesh, India. udaynagapatla@gmail.com. ORCID: 0009-0003-7602-2724.

Volume 6, Issue 14, 2024

Received: 15 June 2024

Accepted: 25 July 2024

Published: 15 Aug 2024

doi:10.48047/AFJBS.6.14.2024.11838-11861

ABSTRACT

In this investigation, we synthesized five novel pyrimidine-benzofuran hybrids by seamlessly merging the pyrimidine and benzofuran motifs, resulting in unique heterocyclic structures. These compounds were meticulously crafted through a well-defined multistep synthesis process, commencing with 5-chlorosalicylaldehyde as the starting material. Rigorous characterization was performed through a comprehensive analysis such as mass spectrometry, 1H NMR spectroscopy, and infrared spectroscopy. By using computational techniques, we were able to predict a number of important characteristics, including drug-likeness, bioactivity scores, toxicity, and the identification of prospective molecular targets, as well as their potential as anti-tubercular and antibacterial agents. We validated these predictions through *in vitro* bioactivity evaluations and Schrödinger docking studies to determine their binding interactions with *Escherichia coli* Topoisomerase IV and *Mycobacterium tuberculosis* enoyl-ACP reductase. Different bacterial strains were employed to investigate the antibacterial efficacy, and the MABA technique was used to analyze the antitubercular activity. Notably, compounds 4c, 4d, and 4e demonstrated significant antitubercular activity, probably, due to the presence of p-chloro, p-methoxy, and p-dimethylamino groups on the aromatic moiety of the pyrimidine ring. Our research highlights the robust antibacterial abilities of these pyrimidine-benzofuran hybrids, which makes them attractive candidates for further lead optimization to produce safer and more potent medications.

Keywords: Pyrimidine Hybrids, Benzofuranyl Chalcones, Anti-tubercular and Antibacterial activities, Molecular Docking.

Introduction

The field of molecular hybrid-based drug discovery is rapidly growing within heterocyclic chemistry. Chemical compounds known as heterocyclic molecular hybrids, which are created by fusing two or more heterocyclic rings, have a wide range of uses in many fields. They are especially prominent in medicinal chemistry, where their intentional design aims to improve the characteristics of pharmaceutical agents [Bérubé , 2016].

The two most important groups of heterocyclic chemicals are benzofurans and pyrimidines [Kabir and Uzzaman, 2022]. Pyrimidines, characterized by two nitrogen atoms in a six-membered ring, have been widely applied in medicine, exhibiting antibacterial [Sirakanyan et al., 2018], anticancer [Abbas et al., 2019], anti-malarial [Mohammad et al., 2021], anti- diabetic [Peytam et al., 2021], anti-HIV [Romeo et al., 2019], and various other notable bioactivities [Patil, 2023].

Conversely, benzofurans have drawn interest due to their potential as pharmacophores in drug design because of their five-membered ring that contains an oxygen atom and their fused benzene ring [Khanam and Shamsuzzaman, 2015]. Many features, such as antitubercular [Bhukya et al., 2020], antibacterial [Xu et al., 2019], antimicrobial [Abbas and Dawood, 2022], antifungal [Mahecha-Mahecha et al., 2023], anti-inflammatory [Chen et al., 2023], anti-cancer [Abbas and Dawood, 2023], and neuroprotective qualities [Dawood, 2019], are well known for these compounds. Pyrimidine-benzofuran hybrids are important because they have the potential to combine the various therapeutic properties of pyrimidines and benzofurans. This presents a promising path for the creation of new pharmaceutical agents that can address a variety of medical needs and further the field of drug discovery and design [Venkatesh et al., 2018; Singh, et al., 2022].

Moreover, benzofuran chalcones constitute a highly significant class of synthetic and biogenetic precursors, found in both synthetic drugs and natural productsA common structural component of many important chemicals used in the pharmaceutical and cosmetics industries is the benzofuran chalcone ring system [Usha and Thangaraj, 2018; Ragab, et al., 2020; Nassar, et al., 2016].

We were motivated to create novel hybrids to explore the synergies of these

pharmacophoric heterocyclics. Our approach involved the synthesis of pyrimidine-benzofuran hybrids by condensing 5-chlorobenzofuranyl chalcone with thiourea, following the traditional method of pyrimidine synthesis involving nucleophiles such as urea, thiourea, or guanidine.

Furthermore, the pressing challenges posed by tuberculosis, bacterial infections, and the unfortunate increase in COVID-19 deaths due to co-infections [TB/COVID-19 Global Study Group, 2022; Daneshvar, et al., 2023; Rajasekhar, et al., 2023] have spurred us to seek innovative solutions. In our pursuit of addressing antibiotic resistance, we were inspired to create hybrids that combine the pharmacophoric qualities of benzofurans and pyrimidines.

To achieve this, we employ *in silico* methods and docking studies, utilizing computational tools to design and optimize these hybrid compounds. *In silico* methods enable us to predict properties, bioactivity scores, and potential molecular targets, including anti-tubercular and antibacterial traits. By using docking experiments, we are able to evaluate the hybrid compounds' binding affinities with important proteins as *Escherichia coli* Topoisomerase IV and Mycobacterium TB enoyl-ACP reductase. This novel method tackles the problems of antibiotic resistance and changing healthcare demands while also speeding up the drug discovery process and advancing the creation of safer and more effective pharmaceutical agents.

Experimental Section

Materials and Methods:

The chemicals we utilized were all purchased from Sigma Aldrich, Hi Media, Qualigens, and Loba suppliers. An open capillary tube digital equipment was used to determine melting points; data are provided unadjusted. UV-visible thin layer chromatography was used to assess purity, and silica gel strips and a hexane, ethyl acetate mobile phase were used. Using KBr disks, a device called SHIMADZU FT-IR 4000 was used to record infrared spectra (υ/cm). An analyzer from the Perkin Elmer Series II 2400 CHNS/O was employed to perform elemental analysis. Using the direct insertion probe approach, mass spectra were collected at 70 eV using a JEOL GC mate II GC-Mass spectrometer. On a BRUKER AVIII-500MHz FT-NMR spectrometer, ^{1}HNMR spectra were obtained using dimethylsulfoxide as the solvent and tetramethylsilane as the internal standard.

Synthetic Procedure:

The synthesis of each molecule in our study is detailed in Scheme 1, beginning with the 5- chlorosalicylaldehyde (1) synthon. This compound was first cyclized to yield 5-chloro-2- acetylbenzofuran (2), the key intermediate. Then, using Claisen-Schmidt condensation, the acetyl group was reacted with different aromatic aldehydes to produce chalcone intermediates (3a–e). Finally, the desired pyrimidine-benzofuran hybrids (4a–e) were obtained by reflux condensation of these chalcones with thiourea in the presence of ethanol and sodium hydroxide.

Scheme 1: General synthetic scheme of pyrimidine-benzofuran hybrids:

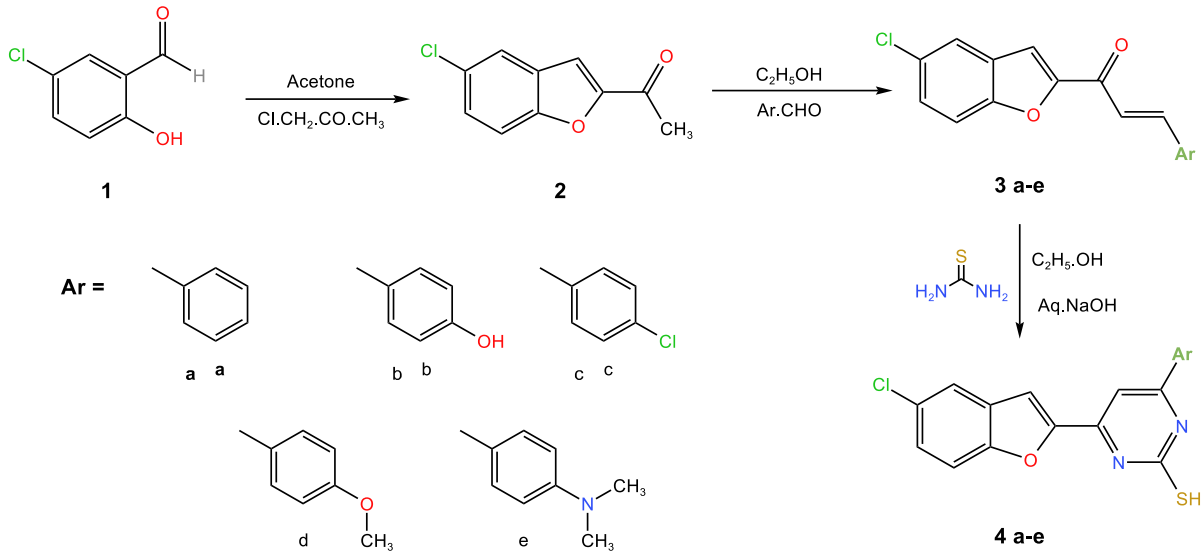

Synthesis of 5-chloro-2-acetylbenzofuran (2):

Over the course of 12 hours, a combination consisting of 5-chlorosalicylaldehyde (1), 5 mL of dry acetone, 4.63 g of chloroacetone, and 15 g of anhydrous potassium carbonate was refluxed. This mixture was filtered once it was finished, and the solvent was removed by concentrating the filtrate under low pressure. 5-chloro-2-acetylbenzofuran (2) was produced by this process and refined further by recrystallization from ethanol. The melting point of the compound was found to be between 83 and 85°C.

General synthesis of chalcones (3a-e):

A cooled solution of 1.94 g of synthon (2) and 0.01 mol of arylaldehyde in 50 mL of ethanol was treated with 5 mL of 70% aqueous sodium hydroxide, added dropwise with continuous stirring. After stirring for an additional 120 minutes, the reaction mixture was left to stand overnight. The resulting solid was neutralized with concentrated hydrochloric acid, collected, and recrystallized from ethanol for purification. The purity of the synthesized compounds, each derived from a different aldehyde, was confirmed using thin-layer chromatography (TLC) with a hexane-ethyl acetate mobile phase.

General synthesis of pyrimidine-benzofuran hybrids:

Anhydrous ethanol (50 mL) was utilized for preparing a solution containing 0.01 mol of thiourea and 0.01 mol of chalcone (3a-e). This solution was refluxed for five hours after 0.01 mol of aqueous sodium hydroxide was added. After completion, the reaction mixture was carefully dumped into cold water. The resultant solid underwent filtration, water washing, and crystallization from ethanol to achieve purification. TLC was used to validate the compound's purity using a hexane acetate mobile phase.

The IUPAC and spectra details of synthesized compounds:

4-(5- Chloro -1-benzofuran-2-yl)-6-phenylpyrimidine-2-thiol (4a): Yield, 80%: m.p.: 138- 140ºC; Anal. calcd. (found) % for C18H11ClN2OS: C, 63.81 (63.88); H, 3.27 (3.35); Cl, 10.46 (10.51); N, 8.27 (8.24); O, 4.72 (4.76); S, 9.46 (9.49); FTIR (νmax, cm–1): 1448 (C=C), 800 (C-Cl), 1568 (C=N); 1H NMR (δ ppm): 7.44-7.69 (5H, 7.50 (d), 7.55 (d), 7.59 (d), 7.64 (d)), 7.89 (1H, d), 8.09 (2H, d), 8.30-8.45 (2H, 8.35 (s), 8.40 (d)), 10.11 (1H,s); MS (m/z, %): 338.02 (M+).

4-[6-(5- Chloro -1-benzofuran-2-yl)-2-mercaptopyrimidin-4-yl]phenol (4b): Yield, 70%: m.p.: 158-160ºC; Anal. calcd. (found) % for C18H11ClN2O2S: C, 60.93 (60.89); H, 3.12 (3.15); Cl, 9.99 (10.05);N, 7.90 (7.93); O, 9.02 (9.06); S, 9.04 (9.09). FTIR (νmax, cm–1): 3741 (O-H), 1433 (C=C), 806 (C-Cl), 1564 (C=N); 1H NMR (δ ppm): 7.18 (2H, d), 7.42-7.64 (2H, 7.47 (d), 7.58 (d)), 7.69-7.99 (4H, 7.75 (d), 7.85 (d), 7.94 (s)), 8.36 (1H, d). 9.82 (1H,d), 10.24 (1H,s); MS (m/z, %): 354.02 (M+).

4-(5- Chloro -1-benzofuran-2-yl)-6-(4-chlorophenyl)pyrimidine-2-thiol (4c): Yield, 75%: m.p.: 167-169ºC; Anal. calcd. (found) % for C18H10Cl2N2OS: C, 57.92 (57.98); H, 2.70 (2.74); Cl, 19.00 (19.06); N, 7.51 (7.54); O, 4.29 (4.32); S, 8.59 (8.61); FTIR (νmax,

cm–1): 1446 (C=C), 796 (C-Cl), 1562 (C=N); 1H NMR (δ ppm): 7.48 (1H, d), 7.60 (1H, d), 7.72-7.98 (5H, 7.79 (d), 7.87 (d), 7.92 (d)), 8.25-8.41 (2H, 8.30 (s), 8.35 (d)), 10.16 (1H,s); MS (m/z, %): 372.98 (M+).

4-(5- Chloro -1-benzofuran-2-yl)-6-(4-methoxyphenyl)pyrimidine-2-thiol (4d): Yield, 72%: m.p.: 152-155ºC; Anal. calcd. (found) % for C19H13ClN2O2S: C, 61.87 (61.92); H, 3.55 (3.53); Cl, 9.61 (9.64);N, 7.60 (7.64); O, 8.68 (8.64); S, 8.69 (8.73); FTIR (νmax, cm–1): 1444 (C=C), 804 (C-Cl), 1547 (C=N); 1H NMR (δ ppm): 3.87 (3H, s), 7.17 (2H, d), 7.42-7.63 (2H, 7.47 (d), 7.57 (d)), 7.68-7.96 (4H, 7.74 (d), 7.84 (d), 7.91 (s)), 8.33 (1H,d), 10.28 (1H,s); MS (m/z, %): 368.03 (M+).

4-(5- Chloro -1-benzofuran-2-yl)-6-[4-(dimethylamino)phenyl]pyrimidine-2-thiol (4e): Yield, 65%: m.p.: 184-187ºC; Anal. calcd. (found) % for C20H16ClN3OS: C, 62.90 (62.88); H, 4.22 (4.26); Cl, 9.28 (9.32);N, 11.00 (11.04); O, 4.19 (4.22); S, 8.40 (8.44); FTIR (νmax, cm–1): 1455 (C=C), 778 (C-Cl), 1565 (C=N); 1HNMR (δ ppm): 2.85 (6H, s), 6.78 (2H, d), 7.40-7.80 (6H, 7.46 (d), 7.53 (d), 7.60 (d), 7.70 (d), 7.75 (s)), 8.29 (1H, d), 10.35 (1H,s); MS (m/z, %): 381.07 (M+).

Prediction of Bioactivity:

Pharmacological activity predictions for the synthesized compounds were carried out using the online tool PASS (Prediction of Activity Spectra for Substances). This tool compares the molecular structures of the synthesized compounds against a comprehensive database of biologically active substances, providing insights into potential bioactivity. By inputting the structural formula or SMILES notation of the title compounds, PASS offered an early-stage prediction of their antibacterial and antitubercular properties, indicating their potential efficacy in these therapeutic areas [Filimonov, et al., 2014].

Molinspiration:

Molinspiration is a valuable resource for the computational chemistry community, offering free online tools for estimating bioactivity scores across various pharmacological targets. This intuitive platform facilitates the analysis of molecular properties and the prediction of bioactivity for a diverse array of chemical compounds. In this study, the Molinspiration web tool was employed to assess the bioactivity of the synthesized title compounds, providing crucial insights into their potential effectiveness against multiple molecular

targets [https://www.molinspiration.com; Zashumo, et al., 2022].

Osiris Property Explorer:

As a fundamental part of Actelion's substance registration system, the Osiris Property Explorer provides real-time computations of properties that are important for drug development. Users can sketch chemical structures, and it instantly calculates properties important to drug development after validation. Drug development is streamlined by making it easier to identify compounds with desirable qualities and potential problems quickly by highlighting traits linked to undesirable consequences in red and those showing drug-like behavior in green [Sander, et al., 2009].

Physicochemical and ADMET Analysis Using Swiss ADME:

The Swiss ADME platform was utilized to analyze the physicochemical properties, drug-likeness, and molecular targets of the synthesized compounds. In addition, *in silico* predictions for absorption, distribution, metabolism, excretion, and toxicity (ADMET) were performed for compounds 4a–e. These evaluations provided valuable insights into the pharmacokinetic profiles and potential safety of the compounds, guiding their suitability as drug candidates [Daina, et al., 2017].

Molecular docking studies:

Preparation of target proteins:

Molecular docking studies were performed to explore the interaction between the synthesized compounds (4a-e) and their target proteins using the GLIDE docking tool (Schrödinger 2020-1) [Friesner, et al., 2006]. The docking process involved two specific crystal structures: the enoyl-ACP reductase from *Mycobacterium tuberculosis* (PDB code: 2PR2) and the 24 kDa subunit of *Escherichia coli* Topoisomerase IV ParE (PDB code: 1S14).

To ensure the accuracy and reliability of the docking studies, several validation tools were employed. ERRAT, Verify 3D, and the Structural Analysis and Verification Server were used to rigorously assess the quality of the selected protein models, confirming their high quality and suitability for docking studies [Eisenberg et al., 1997; Colovos and Yeates, 1993]. Additionally, the RAMPAGE tool was utilized to generate Ramachandran plots, which provided a detailed analysis of the acceptable conformations and dihedral

angles of the protein structures [Lovell et al., 2003].

Preparation of ligand molecules:

The ligand molecules, compounds 4a–e, were initially constructed using ChemDraw Ultra Version 8.0.3 [www.cambridgesoft.com], and the chemical structures were saved in binary format. These structures were then converted to the SDF format using Open Babel GUI version 2.4.1, a versatile molecular modeling application for Windows [https://sourceforge.net/projects/openbabel/files/openbabel/2.4.0/ ; O'Boyle, et al., 2011].

Subsequent energy minimization was performed using the OPLS3e force field via the Ligprep tool. This process included considerations for ionization at a target pH of 7.0±2.0, desalting, and the retention of specific chiralities to ensure the structural integrity of the ligands [Harder, et al., 2016]. In the docking experiments, ATP was employed as the reference ligand to facilitate a comparative evaluation of binding affinities. The binding interactions and docking scores, obtained through GLIDE_SP ligand docking, were meticulously analyzed to determine the potential effectiveness of the synthesized compounds.

Anti-tubercular study:

The microplate Alamar blue test (MABA) was employed to evaluate the antitubercular activity of the synthesized compounds 4a-e, with isoniazide (INH) serving as the reference medication. To prevent evaporation of the medium during the incubation process, the outer wells of a 96-well plate were filled with 200 µL of sterile deionized water. The compounds were directly diluted in a serial manner on the plate, with each well receiving 100 µL of Middlebrook 7H9 (MB 7H9) broth.

The test concentrations for assessing the antitubercular activity ranged from 0.2 to 100 µg/mL. After preparing the plate, it was sealed with Parafilm and incubated at 37°C for five days. Following this incubation period, each well was treated with 25 µL of a freshly prepared 1:1 mixture containing 10% Tween 80 and Alamar blue reagent. The plates were then incubated for an additional day to observe the results. The color change in the wells was used to interpret the outcomes: a pink color indicated bacterial growth, while a blue color signified the absence of bacterial growth [Franzblau, et al., 1998].

Antibacterial study:

The antibacterial activity of the synthesized compounds 4a-e was evaluated using the agar cup plate technique. The assessment was carried out against various bacterial strains, including Gram-positive *Bacillus subtilis* and Gram-negative *Escherichia coli*, with ciprofloxacin serving as the reference standard for comparison in the minimum inhibitory concentration (MIC) evaluation.

Initially, Brain Heart Infusion Agar was brought to room temperature. After transferring the bacterial colonies to the plates, the turbidity of the broth was adjusted to match a vortexed 0.5 McFarland turbidity standard. To ensure uniform distribution, the surface of the agar plate was swabbed three times, with the plate being rotated approximately 60° between each streak. The inoculated plate was then allowed to rest for at least five minutes before the application of the disks.

Using a hot, hollow 5 mm tube, five wells were created in the inoculated agar plate, which were promptly removed. The wells were then filled with varying volumes of the synthesized compounds, 5, 10, 25, 50, and 75µL. After the addition of the compounds, the plates were incubated for 15 minutes, followed by storage at 37°C for 24 hours. The diameter of the inhibitory zones was measured to the nearest millimeter. The MIC procedure involved performing successive dilutions up to 10^{-9} for each compound [Aneja, et al., 2018; CLSI, 2019].

Results and Discussion

Synthesis and characterization:

In this study, we initiated a multi-step synthesis to obtain novel pyrimidinethiol hybrids from 5-chlorobenzofuranyl chalcones using thiourea as a nucleophilic reagent. The process began with the meticulous preparation of the reactants, with 5-chlorosalicylic acid (1) serving as the starting point for the synthesis. This, upon cyclization, resulted in a key synthon, 2-acetyl-5- chlorobenzofuran (2), which, through Claisen-Schmidt condensation reactions with different aryl aldehydes, gave rise to the important intermediates known as chalcones. These compounds were chosen due to their structural significance in pyrimidine synthesis, and they played a central role in the subsequent chemical transformation.

The reaction setup involved the combination of the 5-chlorobenzofuranyl chalcones (3a-

e) with thiourea in an anhydrous ethanol environment. To initiate the reaction, aqueous sodium hydroxide was introduced, setting the stage for a controlled chemical transformation. The refluxing of this mixture for a specific duration, typically 5 hours, was crucial in facilitating the reaction, enabling the conversion of the starting materials into the desired pyrimidinethiol hybrids (4a-e).

The purity of each synthesized compound was confirmed through TLC analysis. TLC was performed using a mobile phase of hexane and ethyl acetate, and each compound exhibited a single distinct spot, indicating a high degree of purity. The Rf values were consistent with the expected outcomes, further confirming the identity of the compounds.

The results from the Infrared (IR) spectra confirmed the presence of the C=N bond in the pyrimidine ring, indicating the successful synthesis of the target compounds (4a-e). In the proton nuclear magnetic resonance (^{1}H NMR) spectra, aromatic protons resonated between 7.1 and 8.4 ppm, while functional groups such as $–OCH_3$ and $–N(CH_3)_2$ appeared at 3.8 and 2.8 ppm, respectively. Remarkably, compound 4b showed a proton singlet at 9.8 ppm, which is indicative of the hydroxy group at the para position of the phenyl ring connected to the pyrimidine system's sixth position. Distinctive - SH group signals were observed around 10.2 ppm. The presence of molecular ion peak (M+) fragments in the mass spectrometry analysis further validated the synthesis and structural integrity of the compounds.

***In silico* profiling:**

Using a large training dataset of 60,000 biologically active chemicals linked to 4,500 different activities, Table 1 shows the biological activity profiles that PASS predicted. The computed probabilities (Pa and Pi) shed light on how likely particular actions are. With Pa values less than 0.5, all substances were initially predicted to have antitubercular properties. Experimental evaluations, however, challenged PASS's predictions by showing notable antitubercular and antibacterial activity, which ran counter to their expectations. In conclusion, PASS anticipates that these compounds will have significant pharmacological potential, especially in the area of antitubercular actions. These hypotheses can be confirmed by additional research, which will expand on the possibility that these molecules are unique pharmacologically active materials.

Table 1: The synthesized compounds bioactivity spectrum predicted by PASS.

Compound	Pa	Pi	Activity
4a	0.573	0.007	Thiol protease inhibitor
	0.485	0.037	Kinase inhibitor
	0.326	0.066	Antimycobacterial
	0.318	0.062	Antituberculosic
4b	0.519	0.010	Thiol protease inhibitor
	0.513	0.032	Kinase inhibitor
	0.345	0.051	Antituberculosic
	0.343	0.058	Antimycobacterial
4c	0.580	0.007	Thiol protease inhibitor
	0.329	0.064	Antimycobacterial
	0.318	0.062	Antituberculosic
	0.289	0.030	Cell wall biosynthesis inhibitor
4d	0.496	0.012	Thiol protease inhibitor
	0.457	0.045	Kinase inhibitor
	0.330	0.064	Antimycobacterial
	0.293	0.074	Antituberculosic
4e	0.454	0.016	Thiol protease inhibitor
	0.361	0.089	Kinase inhibitor
	0.260	0.110	Antimycobacterial
	0.227	0.136	Antituberculosic

As shown in Figure 1, we predicted the bioactivity scores for each produced molecule using Molinspiration. Among the compounds that were produced, compound 4a stood out as an outstanding performer, exhibiting noteworthy bioactivity values. This demonstrates the compounds' significant potential as kinase inhibitors, enzyme inhibitors, and GPCR ligands.

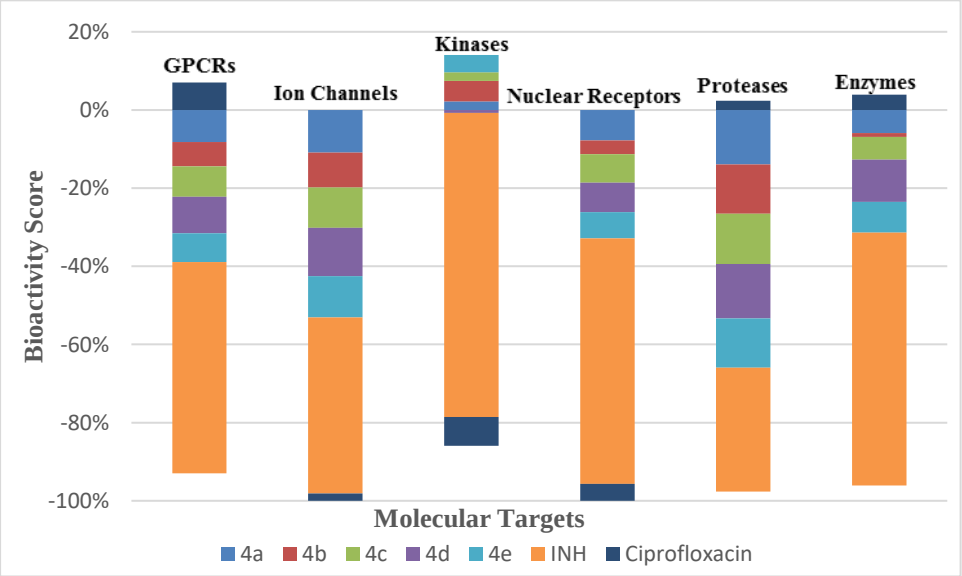

Figure 1: Computation of bioactivity scores using Molinspiration.

An summary of the anticipated toxicological characteristics and drug scores derived from the Osiris Property Explorer is shown in Table 2. Notably, positive drug scores and no significant toxicity issues were predicted for any of the five produced compounds. Compound 4e did, however, show some tumorigenicity potential, which is similar with INH, a common medication. Drug-likeness was evaluated by taking into account a variety of structural and molecular features that show how similar the compounds are to well-known medications. Crucially, every molecule showed great eligibility for therapeutic development, except for compound 4e.

Table 2: Toxicological properties prediction using Osiris.

Compound	**Drug likeness**	**Drug Score**	**MUT[a]**	**TUM[b]**	**IR[c]**	**RT[d]**
4a	-1.53	0.42	--	--	--	--
4b	-1.12	0.46	--	--	--	--
4c	-0.47	0.43	--	--	--	--
4d	-1.08	0.44	--	--	--	--
4e	-1.89	0.24	--	++	--	--
INH	-5.06	0.06	++	++	++	++
Ciprofloxacin	2.07	0.89	--	--	--	--

a=Mutagenicity, b=Tumorigenicity, c=Irritant and d=Reproductive toxicity

The physicochemical, pharmacokinetic, and medicinal chemistry features of the produced compounds were revealed by Swiss ADMET analysis and are briefly reported in Table 3. Notably, every synthesized compound satisfied Lipinski's rule and the necessary conditions for drug-like qualities, such as permissible limits for hydrogen bond donor and acceptor counts, molecular weight, Clog P (lipophilicity), and bioavailability scores (0.55).

Table 3: Swiss ADME-Predicted Properties.

Compound	**GIA[a]**	**BBBP[b]**	**P-gpS[c]**	**LogKp(cm/s)[d]**	**SA[e]**
4a	+++	--	++	-4.76	2.87
4b	+++	--	--	-5.11	2.84
4c	+++	--	++	-4.53	2.88
4d	+++	--	--	-4.96	2.90

4e	+++	--	--	-4.94	3.08
INH	+++	--	--	-7.63	1.23
Ciprofloxacin	+++	--	++	-8.53	3.22

a = Gastrointestinal absorption, b = Blood brain barrier permeant, c = P-gp substrate, d = Skin permeant, e = Synthetic accessibility

Table 3 also highlights that all compounds exhibited favorable pharmacokinetic properties, including strong gastrointestinal absorption and lack of permeability across the blood-brain barrier and skin. Additionally, the support vector machine model confirmed that, with the exception of compounds 4a and 4c, none of the others were predicted to be P-Glycoprotein substrates. The study further demonstrated, using 1024 fragmental contributions (FP2), that compounds 4a–e were readily synthesized, aligning with the reported yields.

The Swiss ADMET platform's thorough examination highlights the potential of the produced chemicals as subjects for additional research in medicinal chemistry and medication development.

Molecular docking studies:

In molecular docking research, it is essential to ensure the quality of 3D models. We employed RAMPAGE's Ramachandran plot analysis to evaluate this. Just 0.9% of the residues in the outlier area, 8.9% in the allowed region, and 89.8% in the favored region were discovered in the protein structure 2PR2. With 94.6% of residues in the desired region, 5.4% in the allowed zone, and 0% in the outlier region, the protein structure 1S14 showed even better results. These near-perfect percentages underscore the exceptional quality and reliability of the predicted models, confirming their suitability for dual-target docking studies (see Figure 2).

To evaluate the structural fidelity of the protein models even more, Verify 3D and ERRAT were used as additional validation methods. The composite quality metrics of 2PR2 and 1S14, which surpass the 95% rejection level, were 94.21% and 95.83%, respectively, according to ERRAT analysis, which confirmed the target protein models' excellence. All of the amino acid residues in 2PR2 showed positive values, according to the Verify 3D study, however some of the residues in 1S14 earned somewhat negative scores. A structurally favorable environment was confirmed by 99.25% of amino acid residues in 2PR2 and 46.43% in 1S14 achieving 3D-1D scores equal to or greater than 0.2, as shown in Figure 3.

Figure 2: Ramachandran plots produced by RAMPAGE for (A) 2PR2 and (B) 1S14, displaying residues in the areas designated as favored (red), allowed (yellow), and outlier (white).

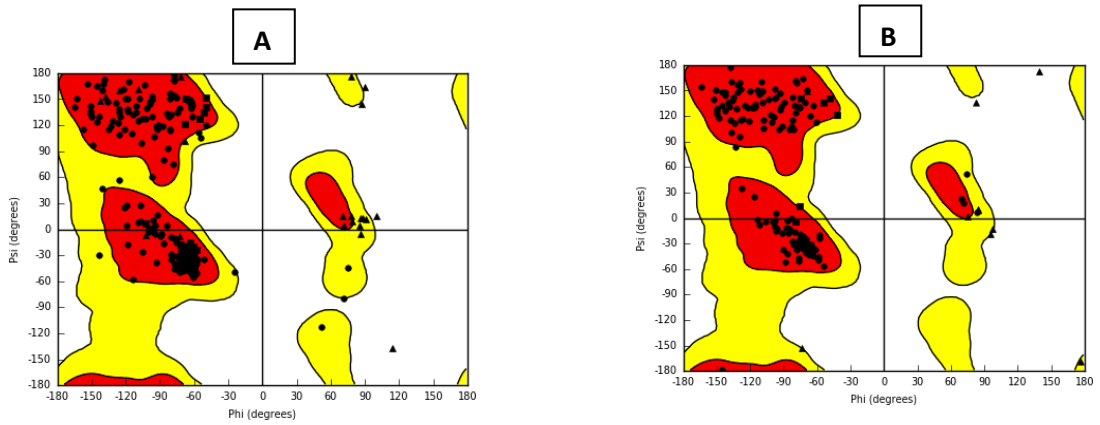

Figure 3. Structural fidelity results of the protein models (A) 2PR2 and (B) 1S14.

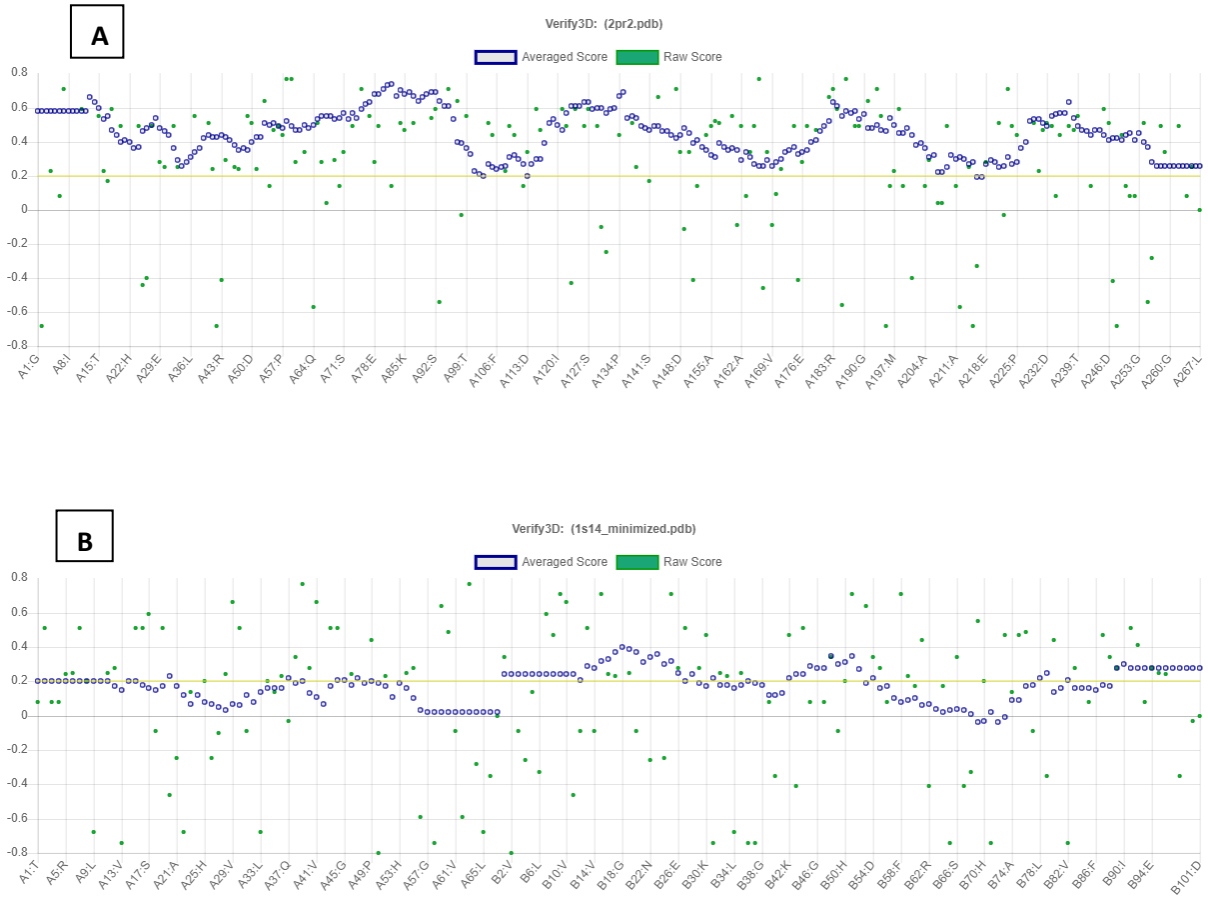

The Schrodinger Glide docking tool was used to estimate the docking score for each ligand contrary to each of the two target proteins. Figures 4 and 5 graphically depict the interaction between compounds 4a–e and the target proteins. Ten binding poses were produced by each docking operation, and the one with the greatest docking value was chosen. Among all the title compounds, compound 4c had the best docking score (-7.748 for 1S14). When compared to the specified standards, all compounds showed acceptable docking scores, suggesting that they could potentially be effective ligands.

Figure 4: Synthesized compounds 4a–e docked with the 2PR2 protein.

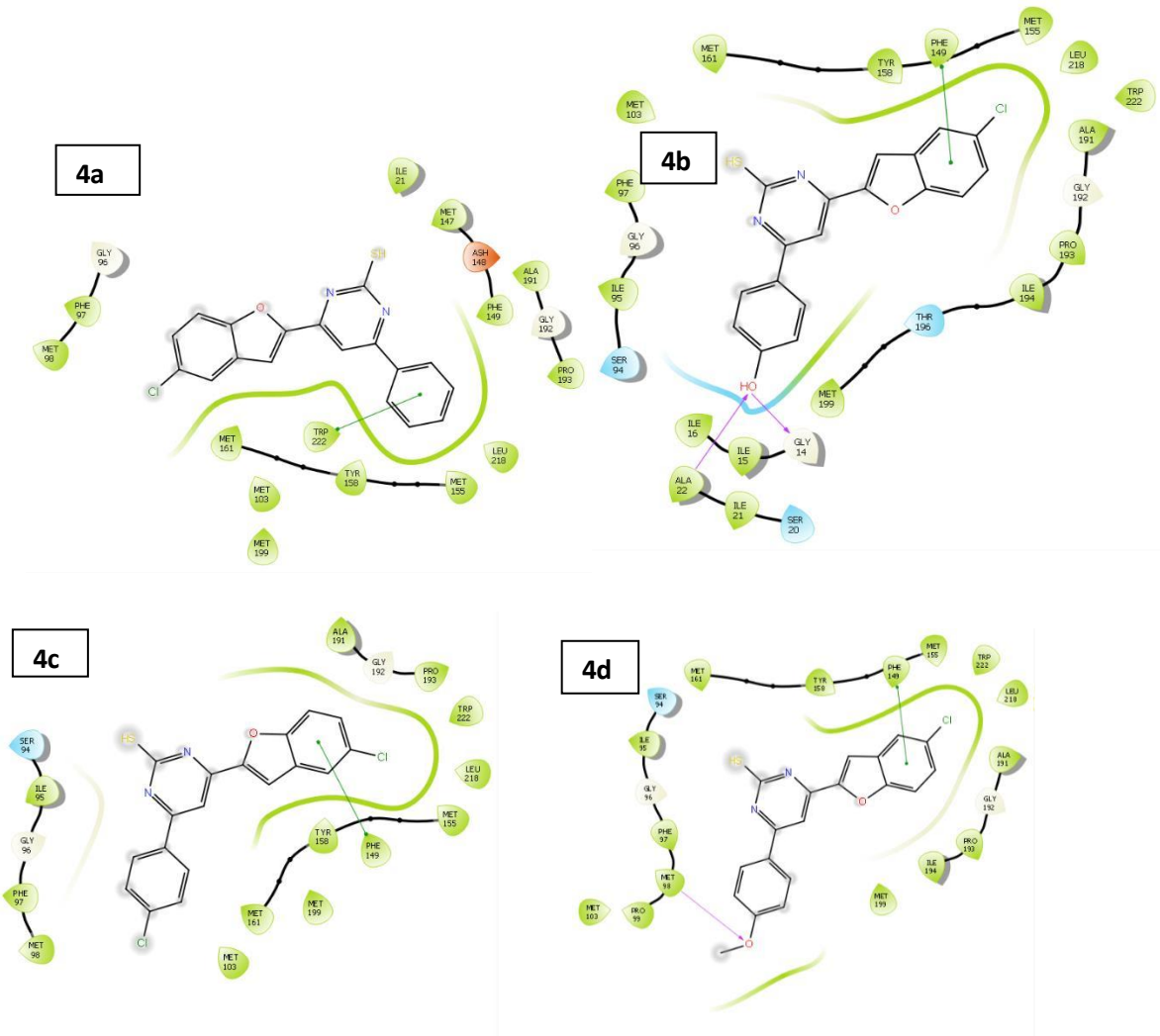

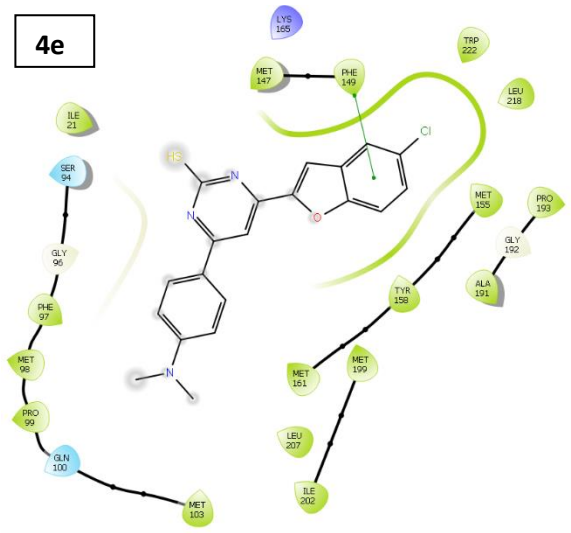

Figure 5: Synthesized compounds 4a–e docked with the 1S14 protein.

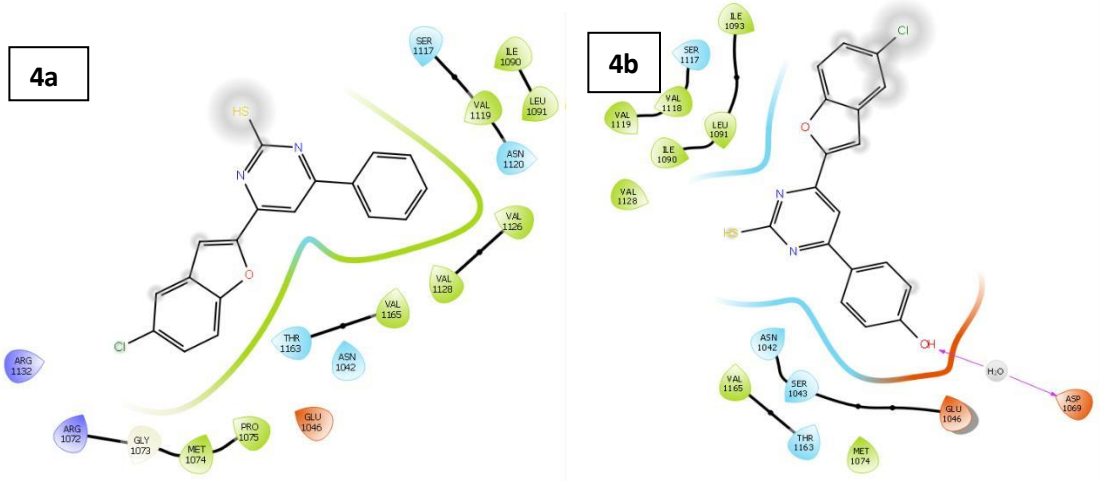

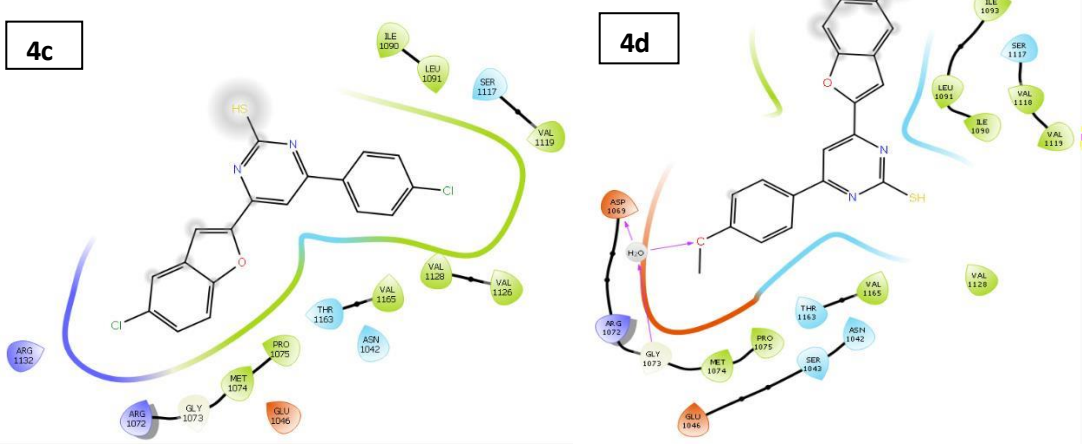

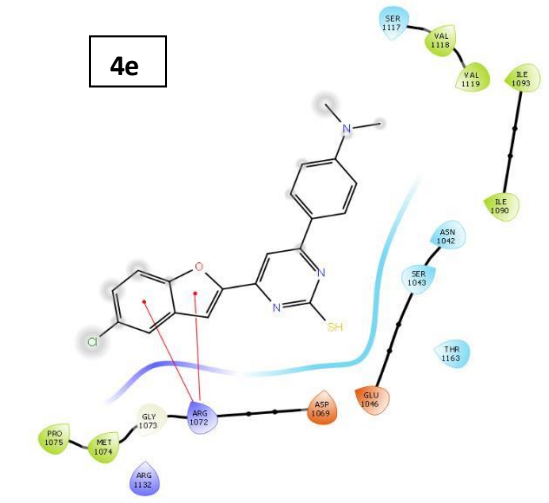

The docking interactions between the ligands and the target proteins 1S14 and 2PR2 are summarized in Tables 4 and 5. Although at distinct interaction locations, compounds 4b, 4c, 4d, and 4e showed hydrophobic interactions with 2PR2 like those of the reference medication INH. Compounds 4a, 4c, and 4e additionally showed hydrogen bond and hydrophobic interactions with 2PR2. Remarkably, all compounds acquired docking scores compared with the reference, confirming similar binding affinities, with the exception of 4a, 4b, and 4d with 2PR2. Interestingly, compounds 4b and 4d also mirrored the hydrogen bond interaction sites of the standard drug with 1S14.

Table 4: Docking interactions and scores of title compounds with the 2PR2 protein.

Compound	Score	Hydrogen Bond Interactions	Hydrophobic Interactions
4a	-8.783	---	TRP 222
4b	-8.543	GLY 14, ALA 22	PHE 149
4c	-7.748	---	PHE 149
4d	-8.195	MET 98	PHE 149
4e	-7.967	---	PHE 149
INH	-7.244	VAL 95, GLY 96	PHE 41

Table 5: Docking interactions and scores of title compounds with the 1S14 protein.

Compound	Score	Hydrogen Bond Interactions	Hydrophobic Interactions
4a	-6.27	---	---
4b	-6.349	ASP 1069	---
4c	-6.191	---	---
4d	-6.026	ASP 1069, GLY 1073	---
4e	-4.904	---	ARG 1072
Ciprofloxacin	-7.066	ASP 1069, GLY 1073	VAL 1118

Antimicrobial studies:

Using INH as the reference medication, all title compounds were evaluated for their antitubercular efficacy against Mycobacterium TB H37Rv in Middlebrook 7H9 broth (refer to Table 6). Compounds 4c, 4d, and 4e, which contain electron-modulating groups such as chloro, methoxy, and dimethylamino at the para position of the aromatic moiety attached to the sixth position of the pyrimidine ring, respectively, showed notable activity at dosages of 25, 50, and 100 µg/mL. In contrast, compounds 4a and 4b showed minimal activity, with limited effect even at 100 µg/mL.

Table 6: Antitubercular activity of title compounds.

Compound	Minimum inhibitory concentration (µg/mL)		
	25	**50**	**100**
4a	Resistant	Resistant	Sensitive
4b	Resistant	Resistant	Sensitive
4c	Sensitive	Sensitive	Sensitive
4d	Sensitive	Sensitive	Sensitive
4e	Sensitive	Sensitive	Sensitive
INH	Sensitive	Sensitive	Sensitive

Employing ciprofloxacin as the reference standard and the agar cup-plate technique, the antibacterial activity of the synthesized compounds (4a–e) was evaluated (refer to Figure 6). Among the examined bacterial strains, compounds 4c and 4d had the strongest antibacterial activity. The p-chloro and p-methoxy groups on the aryl ring at the sixth position of the pyrimidine ring, in particular, are electron-donating substituents that are thought to be responsible for this increased activity.

Notably, all of the compounds showed strong antibacterial action against different strains of bacteria. This is explained by the range of substituents, such as hydroxyl and dimethylamino groups, that are positioned in the para position of the aryl rings. Additionally, their antibacterial qualities were enhanced by the inclusion of the 5-chlorobenzofuran moiety.

Figure 6: Antibacterial activity of title compounds.

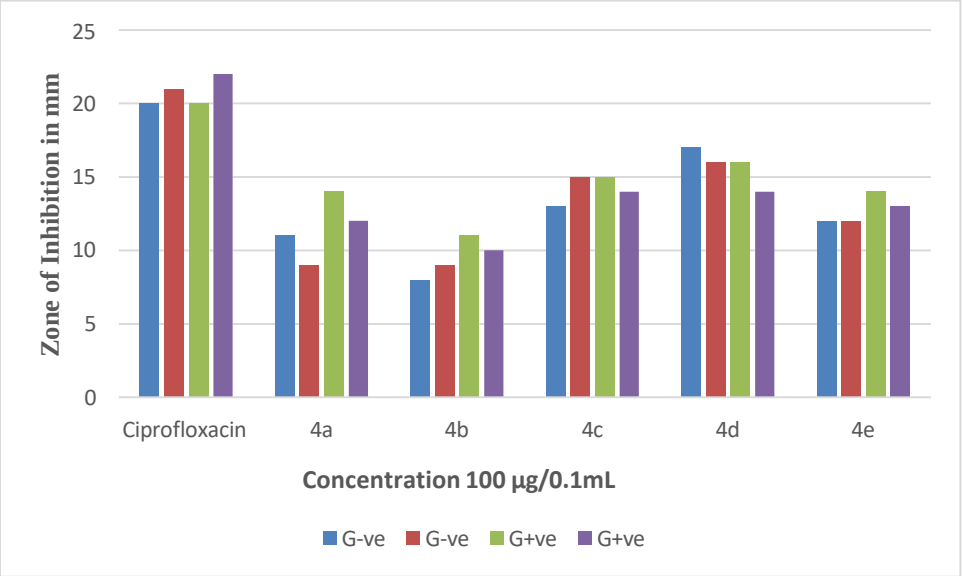

Conclusion:

To sum up, this research explores the synthesis of pyrimidinethiol hybrids and their dual antibacterial properties, emphasizing their potential treatment of bacterial infections and tuberculosis. The chemicals that were produced show great potential in treating various illnesses. Moreover, projections of *in silico* toxicity provide important information about their safety profile.

Moreover, the dual-target docking investigations carried out in this study provide insightful information on how these compounds function to prevent TB and bacterial infections. Comprehending these molecular interactions is critical for addressing the critical problem of multidrug resistant bacteria and establishing the mechanisms of action of the medications.

In summary, this multidisciplinary approach, encompassing organic synthesis,

antimicrobial assessment, molecular docking investigations, and advanced toxicity predictions, provides a holistic perspective on the potential of pyrimidinethiol hybrids. These findings are poised to inspire and guide future research endeavors, propelling innovation in the development of effective antitubercular and antibacterial agents, while ensuring their safety through state-of- the-art toxicity prediction methods. This approach holds the key to addressing the pressing challenges posed by coinfections, tuberculosis, multidrug resistant bacteria, and drug toxicity.

Acknowledgements

The authors are thankful for the research support received from their respective institutions. The Government Dental College and Research Institute in Bellary, India, is especially acknowledged by the authors for their antitubercular evaluation research. The authorities of PASS, Molinspiration, Osiris, and Swiss ADME are also acknowledged by the authors for their kind donations of free software.

References:

1. Bérubé, G. (2016). An overview of molecular hybrids in drug discovery. Expert Opin Drug Discov. 11(3):281-305. https://doi.org/10.1517/17460441.2016.1135125.

2. Kabir, E. and Uzzaman, M. (2022). A review on biological and medicinal impact of heterocyclic compounds, Results in Chemistry, 4, 100606. https://doi.org/10.1016/j.rechem.2022.100606.

3. Sirakanyan, S.N., Geronikaki, A., Spinelli, D. et al. (2018). Synthesis and antimicrobial activity of new amino derivatives of pyrano[4",3":4',5']pyrido[3',2':4,5]thieno[3,2-d]pyrimidine. An Acad Bras Cienc. 2018; 90 (1 Suppl 2):1043-1057. https://doi.org/10.1590/0001-3765201820170798.

4. Abbas, S.E., George, R.F., Samir, E.M.et al. (2019). Synthesis and anticancer activity of some pyrido[2,3-d]pyrimidine derivatives as apoptosis inducers and cyclin-dependent kinase inhibitors. Future Med Chem. 11(18):2395-2414. https://doi.org/10.4155/fmc-2019-0050.

5. Mohammad, M. A., Melati, K., Naziera, M. N. et al. (2021). Synthesis, characterization, docking study and biological evaluation of new chalcone, pyrazoline, and pyrimidine derivatives as potent antimalarial compounds, Arabian Journal of Chemistry, 14 (9), 103304. https://doi.org/10.1016/j.arabjc.2021.103304.

6. Peytam, F., Takalloobanafshi, G., Saadattalab, T. et al. (2021). Design, synthesis,

molecular docking, and in vitro α-glucosidase inhibitory activities of novel 3-amino-2,4-diarylbenzo[4,5]imidazo[1,2-a]pyrimidines against yeast and rat α-glucosidase. Sci Rep. 11(1):11911. https://doi.org/10.1038/s41598-021-91473-z. PMID: 34099819; PMCID: PMC8184976.

7. Romeo, R., Iannazzo, D., Veltri, L. et al. (2019). Pyrimidine 2,4-Diones in the Design of New HIV RT Inhibitors. Molecules. 24(9):1718. https://doi.org/10.3390/molecules24091718.

8. Patil, S.B. (2023). Recent medicinal approaches of novel pyrimidine analogs: A review. Heliyon, **9**, e16773. https://doi:10.1016/j.heliyon.2023.e16773.

9. Khanam, H and Shamsuzzaman. (2015). Bioactive Benzofuran derivatives: A review. European journal of medicinal chemistry, **97**,483–504. https://doi.org/10.1016/j.ejmech.2014.11.039.

10. Bhukya, B., Shukla, A., Chaturvedi, V. et al. (2020). SK. Design, synthesis, in vitro and in silico studies of 2, 3-diaryl benzofuran derivatives as antitubercular agents. Bioorg Chem. 103784. https://doi.org/10.1016/j.bioorg.2020.103784. PMID: 32361184.

11. Xu, Z., Zhao, S., Lv, Z.et al. (2019). Benzofuran derivatives and their anti-tubercular, anti-bacterial activities. European journal of medicinal chemistry, 162:266–276. https://doi.org/10.1016/j.ejmech.2018.11.025.

12. Abbas, A. A. and Dawood, K. M. (2022). Benzofuran as a promising scaffold for the synthesis of novel antimicrobial agents. Expert opinion on drug discovery, 17(12):1357–1376. https://doi.org/10.1080/17460441.2023.2157400.

13. Mahecha-Mahecha, C., Borrego-Muñoz, P., Pombo, L. M. and Gamba-Sánchez, D. (2023). On the way to potential antifungal compounds: synthesis and in vitro activity of 2-benzofuranylacetic acid amides. RSC advances, 13(36):25296–25304. https://doi.org/10.1039/d3ra04737g.

14. Chen, Y., Chen, R., Yuan, R. et al. (2023). Discovery of New Heterocyclic/Benzofuran Hybrids as Potential Anti-Inflammatory Agents: Design, Synthesis, and Evaluation of the Inhibitory Activity of Their Related Inflammatory Factors Based on NF-κB and MAPK Signaling Pathways. International journal of molecular sciences, 24(4):3575. https://doi.org/10.3390/ijms24043575.

15. Abbas, A. A. and Dawood, K. M. (2023). Anticancer therapeutic potential of benzofuran scaffolds. RSC advances, 13(16): 11096–11120. https://doi.org/10.1039/d3ra01383a.

16. Dawood, K. M. (2019). An update on benzofuran inhibitors: a patent review. Expert opinion on therapeutic patents, 29 (11) : 841–870.

https://doi.org/10.1080/13543776.2019.1673727.

17. Venkatesh, T., Bodke, Y.D., Joy, M.N. et al. (2018). Synthesis of Some Benzofuran Derivatives Containing Pyrimidine Moiety as Potent Antimicrobial Agents. Iran J Pharm Res, 17(1):75-86. PMID: 29755540; PMCID: PMC593 7079.

18. Singh, A. K., Kumar, A., Singh, H. et al. (2022). Concept of Hybrid Drugs and Recent Advancements in Anticancer Hybrids. Pharmaceuticals, 15(9):1071. https://doi.org/10.3390/ph15091071.

19. Usha, V. and Thangaraj, V. (2018). Synthesis and Characterisation of Substituted 2-benzofuranyl Chalcones. Materials Today: Proceedings, 5(8): Part 3: 16703-16715. https://doi.org/10.1016/j.matpr.2018.06.034.

20. Ragab, F. A. E., Mohammed, E. I., Abdel Jaleel, et al. (2020). Synthesis of Hydroxybenzofuranyl-pyrazolyl and Hydroxyphenyl-pyrazolyl Chalcones and Their Corresponding Pyrazoline Derivatives as COX Inhibitors, Anti-inflammatory and Gastroprotective Agents. Chemical & pharmaceutical bulletin, 68(8): 742–752. https://doi.org/10.1248/cpb.c20-00193.

21. Nassar, E., El-Badry, Y. A. and El Kazaz, H. (2016). Synthesis, in Vivo Anti-inflammatory, and in Vitro Antimicrobial Activity of New 5-Benzofuranyl Fused Pyrimidines. Chemical & pharmaceutical bulletin, 64(6): 558–563. https://doi.org/10.1248/cpb.c15-00922.

22. TB/COVID-19 Global Study Group. (2022). Tuberculosis and COVID-19 co-infection: description of the global cohort. Eur Respir J, 59(3):2102538. https://doi.org/10.1183/13993003.02538-2021.

23. Daneshvar, P., Hajikhani, B., Sameni, F. et al. (2023). COVID-19 and tuberculosis coinfection: An overview of case reports/case series and meta-analysis of prevalence studies. Heliyon, 9(2):e13637. https://doi:10.1016/j.heliyon.2023.e13637. PMID: 36789387; PMCID: PMC9911156.

24. Rajasekhar, K.K., Guruvareddy, M., Phebe, M. et al. (2023). Design, Synthesis, Anti-tubercular and Docking Studies of Novel 2-Furanyl-3-substituted Quinazolin-4-one Derivatives. Asian J. Chem, 35(3): 617-623. https://doi.org/10.14233/ajchem.2023.27482.

25. Filimonov, D.A., Lagunin, A.A., Gloriozova, T.A. et al. (2014). Prediction of the Biological Activity Spectra of Organic Compounds Using the PASS Online Web Resource. Chemistry of Heterocyclic Compounds, 50:444-457. https://doi.org/10.1007/s10593-014-1496-1.

26. Available from: https://www.molinspiration.com.

27. Zashumo, K.J., Mathivanan, V., Grace, H. et al. (2022). In silico Toxicity Prediction on

Novel Antiobesity Drug Using Cheminformatics Approaches. Int. J. Pharm. Investigation. 12(4):418-22.

28. Sander, T., Freyss, J., von Korff, M. et al. (2009). OSIRIS, an entirely in-house developed drug discovery informatics system. J Chem Inf Model. 49(2):232-246. https://doi.org/10.1021/ci800305f.

29. Daina, A., Michielin, O., Zoete, V. (2017). SwissADME: a free web tool to evaluate pharmacokinetics, drug-likeness and medicinal chemistry friendliness of small molecules. Sci Rep. 7:42717.. https://doi.org/10.1038/srep42717.

30. Friesner, R.A., Murphy, R.B., Repasky, M.P. et al. (2006). Extra Precision Glide: Docking and Scoring Incorporating a Model of Hydrophobic Enclosure for Protein−Ligand Complexes. J. Med. Chem, 49, 6177– 6196; https://doi.org/10.1021/jm051256o.

31. Eisenberg, D., Lüthy, R. and Bowie, J. U. (1997). VERIFY3D: assessment of protein models with three-dimensional profiles. Methods in enzymology, 277:396–404. https://doi.org/10.1016/s0076-6879(97)77022-8.

32. Colovos, C. and Yeates, T. O. (1993). Verification of protein structures: patterns of nonbonded atomic interactions. Protein science : a publication of the Protein Society, 2(9): 1511–1519. https://doi.org/10.1002/pro.5560020916.

33. Structural Analysis, Verification Server. (2011). Available from: http://nihserver. mbi.ucla. edu/SAVES/.

34. Lovell, S.C., Davis, I.W., Arendall 3rd, W.B. et al. (2003). Structure validation by Cα geometry: ϕ,ψ and Cβ deviation. Proteins, 50(3): 437–450. https://doi.org/10.1002/prot.10286.

35. Cambridge Soft Corporation, a subsidiary of PerkinElmer, Inc. (2014). Chem DrawUltra version 8.0.3 for Windows. Available from: www.cambridgesoft.com.

36. https://sourceforge.net/projects/openbabel/files/openbabel/2.4.0/. License: GNU GPL v2.

37. O'Boyle, N. M., Banck, M., James, C. A. et al. (2011). Open Babel: An open chemical toolbox. *Journal of cheminformatics*, 3:33. https://doi.org/10.1186/1758-2946-3-33.

38. Harder, E., Damm, W., Maple, J. et al. (2016). OPLS3: A Force Field Providing Broad Coverage of Drug-like Small Molecules and Proteins. Journal of chemical theory and computation, 12(1): 281–296. https://doi.org/10.1021/acs.jctc.5b00864.

39. Franzblau, S. G., Witzig, R. S., McLaughlin, J. C. et al. (1998). Rapid, low-technology MIC determination with clinical Mycobacterium tuberculosis isolates by using the microplate Alamar Blue assay. Journal of clinical microbiology, 36(2):362–366. https://doi.org/10.1128/JCM.36.2.362-366.1998.

40. Aneja, B., Azam, M., Alam, S. et al. (2018). Natural Product-Based 1,2,3-

Triazole/Sulfonate Analogues as Potential Chemotherapeutic Agents for Bacterial Infections. ACS Omega. 3:6912–6930, (2018). https://doi.org/10.1021/acsomega.8b00582.

41. CLSI. (2019). M100 Performance Standards for Antimicrobial Susceptibility Testing. 29th ed. CLSI; Wayne, PA, USA.